



Article (refereed) – Published version

Williams, Charlotte; Sharples, Jonathan; Mahaffey, Claire; Rippeth, Tom. 2013 Wind-driven nutrient pulses to the subsurface chlorophyll maximum in seasonally stratified shelf seas. *Geophysical Research Letters*, 40 (20). 5467-5472.

[10.1002/2013GL058171](https://doi.org/10.1002/2013GL058171)

This version available at <http://nora.nerc.ac.uk/504200/>

NERC has developed NORA to enable users to access research outputs wholly or partially funded by NERC. Copyright and other rights for material on this site are retained by the rights owners. Users should read the terms and conditions of use of this material at

<http://nora.nerc.ac.uk/policies.html#access>

AGU Publisher statement: An edited version of this paper was published by AGU. Copyright (2013) American Geophysical Union. Further reproduction or electronic distribution is not permitted.

Williams, Charlotte; Sharples, Jonathan; Mahaffey, Claire; Rippeth, Tom. 2013 Wind-driven nutrient pulses to the subsurface chlorophyll maximum in seasonally stratified shelf seas. *Geophysical Research Letters*, 40 (20). 5467-5472. [10.1002/2013GL058171](https://doi.org/10.1002/2013GL058171)

To view the published open abstract, go to <http://dx.doi.org/10.1002/2013GL058171>

Contact NOC NORA team at
publications@noc.soton.ac.uk

Wind-driven nutrient pulses to the subsurface chlorophyll maximum in seasonally stratified shelf seas

Charlotte Williams,^{1,2} Jonathan Sharples,^{1,2} Claire Mahaffey,¹ and Tom Rippeth¹

Received 7 October 2013; accepted 10 October 2013; published 28 October 2013.

[1] Shelf seas are an important global carbon sink. In the seasonal thermocline, the subsurface chlorophyll maximum (SCM) supports almost half of summer shelf production. Using observations from the seasonally stratified Celtic Sea (June 2010), we identify wind-driven inertial oscillations as a mechanism for supplying the SCM with the nitrate needed for phytoplankton growth and carbon fixation. Analysis of wind, currents, and turbulent dissipation indicates that inertial oscillations are triggered by a change in the wind velocity. High magnitude, short-lived dissipation spikes occur when the shear and wind vectors align, increasing the daily nitrate flux to the SCM by a factor of at least 17. However, it is likely that the sampling resolution of turbulent dissipation does not always capture the maximum wind-driven peak in mixing. We estimate that wind-driven inertial oscillations supply the SCM with ~33% to 71% of the nitrate required for new production in shelf seas during summer. **Citation:** Williams, C., J. Sharples, C. Mahaffey, and T. Rippeth (2013), Wind-driven nutrient pulses to the subsurface chlorophyll maximum in seasonally stratified shelf seas, *Geophys. Res. Lett.*, 40, 5467–5472, doi:10.1002/2013GL058171.

1. Introduction

[2] Shelf seas are regions of high biological activity, disproportionately contributing 15–30% of the global oceanic primary production [Wollast, 1998] while occupying only 8% of the global ocean surface area. Temperate shelf seas have been implicated as substantial sinks for atmospheric carbon dioxide (CO₂) at the sea surface [Thomas *et al.*, 2004; Borges *et al.*, 2005; Jahnke, 2010]. The carbon sequestration capability of European shelf seas has been particularly well documented [Frankignoulle and Borges, 2001; Borges *et al.*, 2006]. In these shelf seas annual primary production is partitioned approximately equally between the relatively short duration spring bloom and weaker but more sustained growth in the subsurface chlorophyll maximum (SCM) within the base of the seasonal thermocline through the summer [Hickman *et al.*, 2012], with a deficit in sea surface pCO₂ correlated to the chlorophyll concentration in the SCM [Kitidis *et al.*, 2012]. The diapycnal nutrient flux from the bottom mixed layer (BML) to the SCM sets a limit on summer new production [e.g., Sharples *et al.*, 2001].

Observations of vertical nitrate fluxes in shelf seas have demonstrated typical background rates of 1–2 mmol m⁻² d⁻¹ [e.g., Sharples *et al.*, 2001; Williams *et al.*, 2013], which can be augmented significantly by topographically driven internal waves [e.g., Sharples *et al.*, 2007; Lucas *et al.*, 2011; Tweddle *et al.*, 2013]. Shear and instabilities at the thermocline arising from wind-driven inertial oscillations potentially provide another mechanism for generating a vertical turbulent nitrate flux [Rippeth, 2005; Rippeth *et al.*, 2005]. These inertial oscillations are generated by a sudden change in wind forcing which causes the surface layer to oscillate horizontally over the bottom mixed layer at the inertial frequency [e.g., Pollard, 1980; Itsweire and Hellend, 1989]. They have been observed and extensively reviewed in the scientific literature [e.g., van Haren *et al.*, 1999; Knight *et al.*, 2002] and identified as an important mechanism in the vertical advection of nutrient-rich deep water in the coastal zone [Lucas *et al.*, 2013]. However, current shear and mixing generated by this slab-like motion of the surface layer is thought to occur in short-lived spikes, when the wind and shear vectors are aligned [Burchard and Rippeth, 2009]. Here we present observations of vertical turbulent nitrate fluxes during contrasting periods of calm weather and strong winds, thus demonstrating the large impact that winds can have on daily rates of nitrate supply to the SCM. We show that the increased nitrate flux is dominated by a few very short bursts of turbulence. Moreover, we use these observations to estimate the likely contribution that episodic wind events could have on the primary production in a temperate shelf system.

2. Methods

[3] Measurements were collected from the *RRS Discovery* (cruise D352) during neap tides at a station in the Celtic Sea located on the NW European shelf at station IM1 (Figure 1; 49°25'N, 08°58'W). The sampling campaign, (decimal days 156 to 161 in 2010) consisted of measurements of vertical profiles of turbulent kinetic energy dissipation, water and wind velocity, inorganic nutrients, and chlorophyll *a* (hereafter chl *a*).

2.1. Water Column Structure, Chlorophyll *a* and Inorganic Nutrients

[4] A rosette frame, supporting a Seabird 911 conductivity, depth, temperature (CTD) instrument, a Chelsea Instruments Aquatrack MkIII fluorometer and 10 L Niskin bottles, was used to collect vertical profiles (e.g., Figure 1b) of salinity, temperature, chl *a* fluorescence, and seawater samples. Seawater samples were analyzed onboard the vessel for inorganic nutrients and extracted chl *a* concentrations. Inorganic nutrient concentrations were determined using a Bran and Luebbe QuAAtro five-channel segmented flow nutrient analyzer. Discrete measurements of chl *a* were

¹School of Environmental Sciences, University of Liverpool, Liverpool, UK.

²National Oceanography Centre, Liverpool, UK.

³School of Ocean Sciences, Bangor University, Menai Bridge, UK.

Corresponding author: C. Williams, School of Environmental Sciences, University of Liverpool, Liverpool L69 3GP, UK. (cwill8@liv.ac.uk)

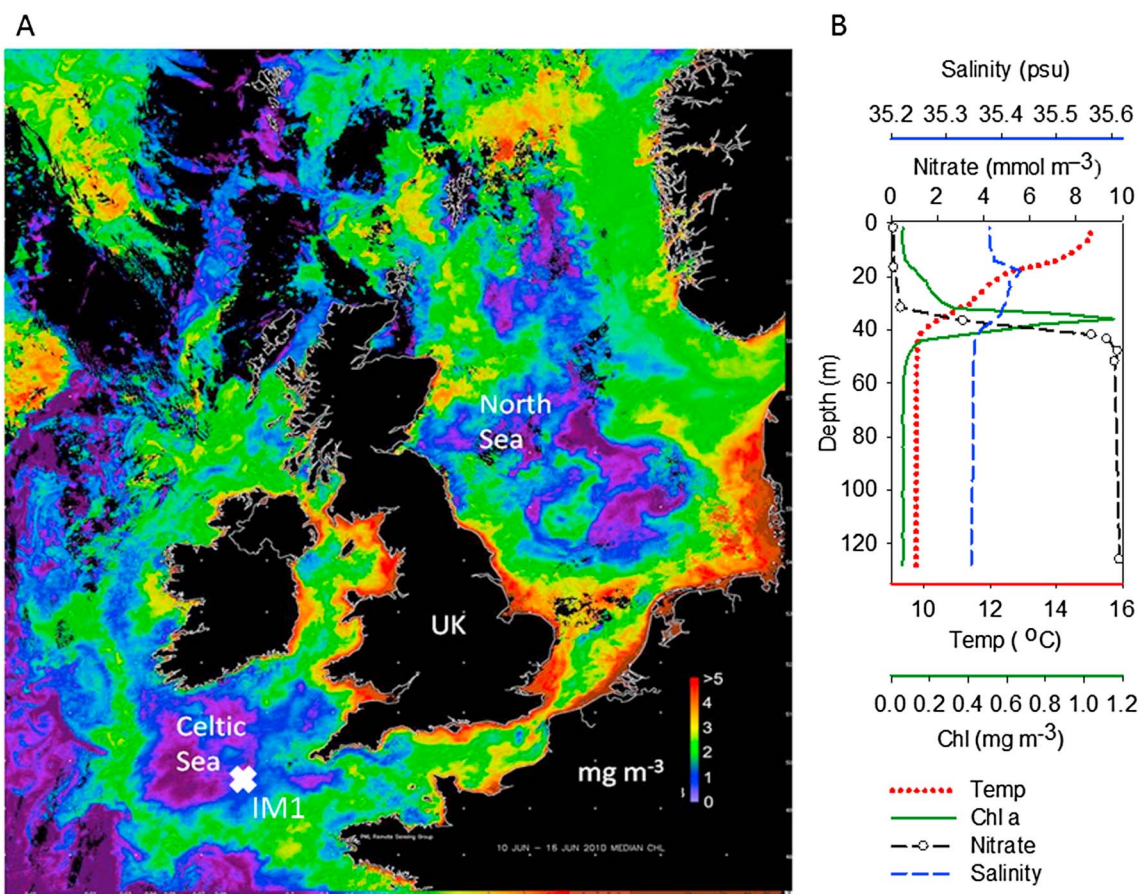


Figure 1. (a) Sea surface chlorophyll composite from 10–16 June 2010 showing the Celtic Sea and sampling station IM1 (indicated by white cross; image courtesy of NEODAAS). (b) Typical profile of nitrate (dashed line with open circle), chlorophyll *a* (green solid line), temperature (red dotted line), and salinity (blue dashed line) from CTD 007 (6 June 2010 at 02:31 h), showing that the position of the subsurface chlorophyll maximum corresponds to the base of the thermocline and a sharp nitrate gradient.

determined by filtering 1 L of seawater onto a Whatman glass fiber filter (GF/F) and extracting with acetone. Fluorescence was determined against chl *a* using a Turner TD-700 fluorometer [Evans *et al.*, 1987]. The extracted chl *a* concentrations were used to calibrate the fluorescence sensor, with calibration having a root mean square deviation of $\pm 0.1 \text{ mg m}^{-3}$.

2.2. Turbulence and Vertical Structure of the Water Column

[5] Vertical profiles of velocity microstructure, temperature and salinity were collected over two sampling campaigns (days 156 to 158, and 160 to 161) using a Rockland Oceanographic VMP500 Velocity Microstructure Profiler. Profiles were taken continuously during each time series, with each down-up profile taking approximately 10 min. Interruptions to the time series occurred due to either ship repositioning or a conductivity-temperature-depth (CTD) operation. The microstructure velocity shear measured from the VMP500 was used to calculate the dissipation of turbulent kinetic energy (TKE), ϵ , following Rippeth *et al.* [2003].

2.3. Meteorology and Tidal Currents

[6] Meteorological and current data were collected from a mooring at the IM1 station. A surface toroid buoy was fitted with an Airmar PB200 meteorological sensor package, and

recorded 10 min averages of wind speed and direction, which were used to calculate the wind stress at the sea surface. An upward-looking 150 kHz acoustic Doppler current profiler (ADCP), attached to a frame on the seabed, measured components of velocity through the water column at 2 m vertical resolution and averaged every 2 min. The difference in velocity of both components at each depth bin within the thermocline was used to calculate the mean interfacial shear squared term ($S^2 = (du/dz)^2$). This interfacial shear was calculated using the vertical difference in the two horizontal velocity components [e.g., Burchard and Rippeth, 2009]. The weather station on the surface buoy recorded 10 min averages of wind speed and direction, which were used to calculate the wind stress at the sea surface.

2.4. Flux Calculations

[7] Nitrate fluxes were calculated from TKE dissipation and nitrate concentrations following Sharples *et al.* [2007], with means and 95% confidence intervals estimated using a Gaussian bootstrap resampling method [Efron and Gong, 1983]. If the rate of the turbulent nitrate supply into the SCM is greater than the nitrate uptake rate by phytoplankton in the SCM, nitrate from the BML may be mixed through the thermocline and into the surface layer. Thus, estimating the nitrate flux out of the upper thermocline and into the SML

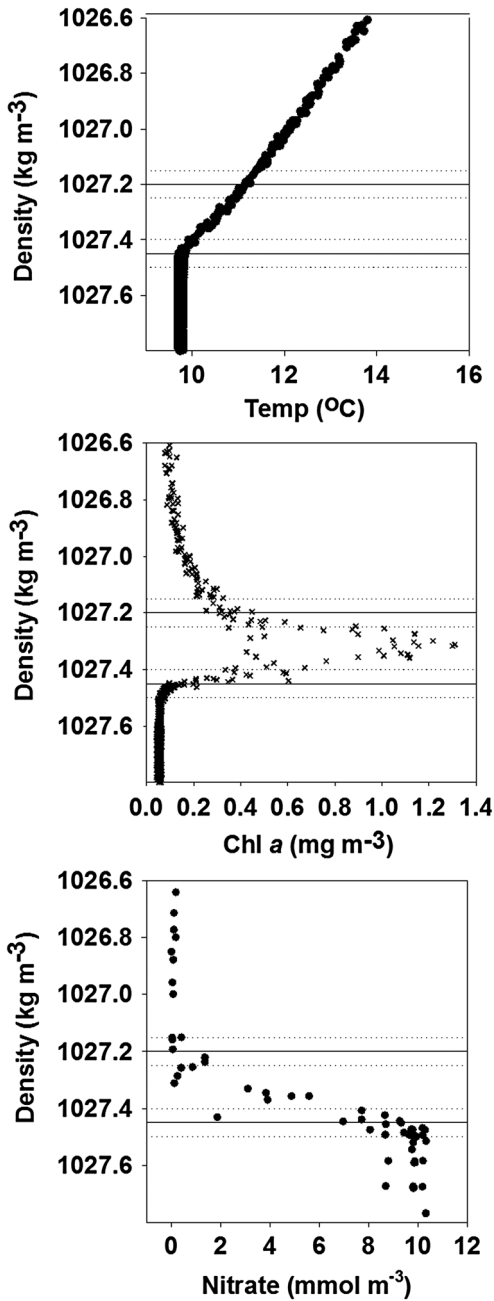


Figure 2. (top) Temperature ($^{\circ}\text{C}$) versus density (kg m^{-3}) measured from the CTD profiles during the VMP sampling campaign. (middle) Chlorophyll *a* (mg m^{-3}) versus density (kg m^{-3}) measurements during the VMP sampling period. (bottom) Nitrate (mmol m^{-3}) concentration relative to density values (kg m^{-3}). The nitrate-density gradients at the top and base of the thermocline were 19.74 and $40.32 \text{ mmol m}^{-4}$, respectively. The solid lines mark the $1027.2 (\pm 0.05) \text{ kg m}^{-3}$ and $1027.45 (\pm 0.05) \text{ kg m}^{-3}$ (marked by dotted lines isopycnals), which describe the density band marking the top and base of the SCM where fluxes were calculated over respectively.

is also of interest, as it provides an indication of whether the rate of nitrate assimilation by phytoplankton in the SCM exceeds the rate of nitrate transport from the BML via turbulent mixing. In order to correctly identify the thermocline base

and top accurately, we calculated the fluxes across fixed isopycnals rather than fixed depths. The base of the nitracline was defined as the $1025.2 (\pm 0.05) \text{ kg m}^{-3}$ and the top of the nitracline as the $1025.45 (\pm 0.05) \text{ kg m}^{-3}$ (Figure 2, top). The density-nitrate relationships at the top and base of the nitracline were calculated within these isopycnal bands (Figure 2, bottom) and were statistically robust ($R^2 = 0.68$ and 0.83 , respectively, $p < 0.0001$). The “background” nitrate flux was estimated from the second VMP sampling campaign taken during low winds. The wind-driven nitrate flux is described in the results and was estimated over the initial 50 h VMP sampling period during enhanced winds.

3. Results and Discussion

3.1. Water Column Structure

[8] The thermocline was typically 30 m thick in all profiles, and vertical salinity variations were small (< 0.1 (PSS)) so that the density structure was driven primarily by temperature variations (Figure 2, top). The isopycnals encompassing the SCM covered a vertical range of up to 15 m (Figure 2, middle). The thermocline consistently coincided with the SCM peak, the position of which varied vertically between depths of 35 to 50 m. An SCM was evident in all CTD casts before, during, and after the wind mixing event. The concentration of the SCM peak varied considerably throughout all CTD profiles (0.4 to 1.4 mg m^{-3}), indicating either horizontal patches of chl *a* or the turbulent erosion of phytoplankton from the SCM via vertical mixing. Surface chl *a* concentrations were consistently below 0.05 mg m^{-3} , and nitrate concentrations were below the limit of detection (0.1 mmol m^{-3}). The bottom mixed layer was replete in inorganic nutrients; nitrate concentrations were relatively stable at a concentration of 9.5 to 10 mmol m^{-3} below the nitracline. The nitracline was observed to correspond with the SCM peak (Figure 2).

3.2. Wind-Driven Mixing

[9] Wind data from the IM1 mooring indicated a pronounced increase in wind stress from $< 0.05 \text{ N m}^{-2}$ (wind velocity $< 5 \text{ m s}^{-1}$) on day 156 to 0.10 N m^{-2} (wind velocity $= 8 \text{ m s}^{-1}$) on day 157, with a wind stress peak exceeding 0.25 N m^{-2} (wind velocity $> 12 \text{ m s}^{-1}$) on day 158 (Figure 3a). Shear magnitude (s^{-2}) at the base of the thermocline appeared to oscillate between $6 \times 10^{-4} \text{ s}^{-2}$ and $< 1 \times 10^{-4} \text{ s}^{-2}$ with a frequency of 12 to 15 h (Figure 3c). Intermittent spikes of high dissipation within the thermocline occurred during the initial VMP time series (days 156–158) and ranged between 1×10^{-7} and $1 \times 10^{-5} \text{ m}^2 \text{ s}^{-3}$ (Figure 3d); these spikes have been annotated as J, K, L, and M on Figure 3d. Dissipation within the thermocline was strongly intermittent, varying by more than two orders of magnitude (Figure 3d). The largest observed mixing event during the first VMP time series occurred on day 157.4 (event K), with a dissipation rate of $6 \times 10^{-5} \text{ m}^2 \text{ s}^{-3}$, more than two orders of magnitude larger than the other mixing events observed (J, L, and M). Turbulent kinetic energy dissipation events corresponded with periods of enhanced shear (Figure 3c and J, K, L, and M on Figure 3d). Interestingly, we failed to sample turbulent kinetic energy dissipation during the strongest shear event (just after day 159.0). The largest mixing event observed (event K) could be interpreted as anomalous; however, it appears consistent with measurements immediately before and after it and is made

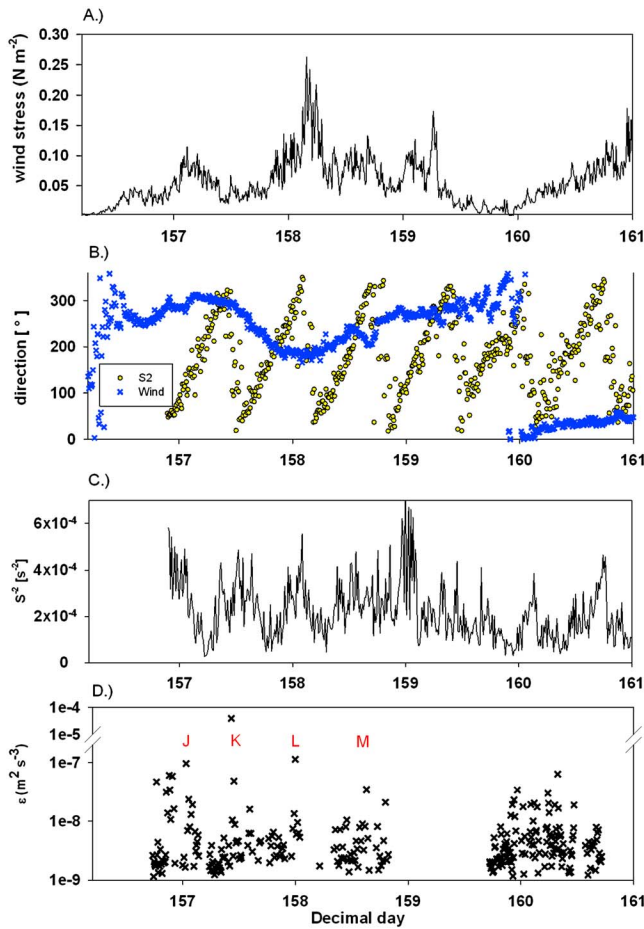


Figure 3. (a) Wind stress calculated from the 10 min time-averaged wind speed (m s^{-1}) measured from the Airmar PB200 weather station on the surface buoy at IM1. (b) Direction ($^{\circ}$) of the interfacial shear (10 min smoothed) within the thermocline (dots) and the wind vector (crosses). (c) Instantaneous \log_{10} dissipation of turbulent kinetic energy, ϵ , within the thermocline ($\text{m}^2 \text{s}^{-3}$). All measurements were taken at station IM1 in the Celtic Sea ($49^{\circ}25'N$, $08^{\circ}58'W$) during decimal days 156.8–160.8 (6–8 June) in 2010.

up of seven individual dissipation values within the isopycnal band. Confidence in event K implies that large dissipation peaks are extremely short-lived and difficult to resolve, even with the continuously profiling VMP. It is therefore possible that we may have underestimated the magnitude of spikes in dissipation during event L and M. Following *Burchard and Rippeth* [2009], analysis of the shear and wind vectors demonstrated that the alignments of the wind direction and the shear directions corresponded to spikes in diapycnal mixing across the thermocline during three of the four mixing events within the first

VMP time series (K, L, and M). Furthermore, the shear vector within the thermocline was seen to rotate in a clockwise direction at close to the inertial frequency following an increase in the wind speed on day 157. Wind-driven inertial mixing events are believed to be separated by the local inertial frequency if the wind direction stays the same. Mixing events K and L, and L and M (Figure 3d) were separated by a period of approximately 15 h corresponding to the local inertial frequency at this latitude (15.7 h) while the wind direction was blowing toward the south. There was a consistent lag in diapycnal mixing events, with peak mixing occurring approximately 1.5 to 3 h after the initial shear-wind alignment. This lag was due to maximum shear occurring when the rate of shear growth switches from positive to negative (i.e., $=0$), which occurs 90° after the wind vector and shear vector alignment [*Burchard and Rippeth*, 2009]. Thus, shear production will have occurred throughout the shear-wind alignment, eventually resulting in shear instabilities and subsequent mixing following the alignment. A change in the wind forcing at the beginning of the time series generated inertial oscillations in the surface layer, where the alignment of the wind and shear vectors appeared to result in periods of enhanced shear at the thermocline. Several dissipation events occurred at the beginning of the time series (event J) coinciding with a period of high shear. Current data before event J was unavailable; this enhanced shear and dissipation may have been the result of a wind-shear vector alignment that occurred when no ADCP measurements were available (pre-day 157).

[10] During the second VMP time series, no clear separated spikes of dissipation from the background dissipation were observed as the wind stress increased from calm to 0.08 N m^{-2} (Figure 3d). The dissipation of turbulent kinetic energy remained between 1×10^{-9} and $1 \times 10^{-8} \text{ m}^2 \text{ s}^{-3}$ for the duration of the second VMP time series.

3.2.1. Nitrate Fluxes

[11] The daily background supply of nitrate to the base of the thermocline was calculated during the second VMP time series (day 160) as 1.3 (95% CI = 1.0 to 1.6) $\text{mmol m}^{-2} \text{ d}^{-1}$, which was consistent with the canonical nitrate flux estimates of 1 to 2 $\text{mmol m}^{-2} \text{ d}^{-1}$ for northwest European shelf seas [*Sharples et al.*, 2001, 2007; *Rippeth et al.*, 2009]. Assuming the Redfield C:N ratio of 6.6 [*Redfield*, 1958], this flux is capable of supporting $105 \text{ mg C m}^{-2} \text{ d}^{-1}$ of new production (Table 1). Estimates of euphotic zone depth integrated total primary production from this period were between 174 and $386 \text{ mg C m}^{-2} \text{ d}^{-1}$ [*Hickman et al.*, 2012]. The background turbulent supply of nitrate was capable of supporting 27 to 60% of the total primary production observed in the euphotic zone, implying that the remaining production was regenerated. During enhanced winds, however, the nitrate flux into the base of the thermocline increased almost 17-fold to 22 (2 to 81) $\text{mmol m}^{-2} \text{ d}^{-1}$. This flux would be capable of supporting 1735 (166 to 6404) $\text{mg C m}^{-2} \text{ d}^{-1}$ of new production. The wind-driven

Table 1. Daily Wind-Driven and Background Nitrate Fluxes^a

Flux	Top of Thermocline	Base of Thermocline
Daily background nitrate flux ($\text{mmol m}^{-2} \text{ d}^{-1}$)	0.2 (0.1–0.2)	1.3 (1.0–1.6)
Background potential nitrate driven production ($\text{mg C m}^{-2} \text{ d}^{-1}$)	13 (10–15)	105 (82–128)
Daily nitrate flux during enhanced winds ($\text{mmol m}^{-2} \text{ d}^{-1}$)	0.3 (0.2–0.6)	22 (2–81)
Potential nitrate driven production during enhanced winds ($\text{mg C m}^{-2} \text{ d}^{-1}$)	23.8 (12–48)	1735 (166–6404)

^aDaily nitrate fluxes ($\text{mmol m}^{-2} \text{ d}^{-1}$) into the top and base of the nitracline, during both low and enhanced winds (with and without spike J described in Figure 6). Daily nitrate fluxes have been converted into potential nitrate driven production using the Redfield ratio ($\text{mg C m}^{-2} \text{ d}^{-1}$).

nitrate flux, therefore, provided between 500 (43 to 1659)% and 1000 (95 to 3680)% of the nitrogen needed to support the total PP that has been observed in the Celtic Sea, and thus the wind is an important, perhaps essential, supplier of nitrate to the SCM. If mixing events K, L, and M are omitted from the flux calculation, the daily nitrate flux was 3 (2 to 4) mmol m⁻² d⁻¹, which is of a similar magnitude to the canonical shelf sea nitrate flux estimates [e.g., *Sharples et al.*, 2001, 2007; *Rippeth et al.*, 2009; *Williams et al.*, 2013], as well as our estimate during low wind and no enhanced dissipation events (Table 1). Thus, high dissipation events induced by shear spikes drive the high nitrate flux which is only observed during the periods of high wind.

[12] Only a small amount of the nitrate supplied from the BML appears to be either surplus to phytoplankton nitrogen requirements and/or is not assimilated quickly by phytoplankton in the SCM, and hence a small amount was able to reach the SML (0.3 mmol m⁻² d⁻¹; Table 1). This indicates that potentially 500 to 1000% of the nitrate that is estimated to be required for production may have been assimilated by phytoplankton within the SCM. The intermittent mix events were observed at the base of the thermocline, but not at the top into the nitrate deplete surface layer. However, the small increase in nitrate supplied to the SML during enhanced winds was equivalent to a twofold increase in new production (13 to 24 mg C m⁻² d⁻¹; Table 1).

[13] The increase in nitrate supplied to the surface during enhanced winds was not observed in the surface nitrate concentrations, which were consistently <0.1 mmol m⁻³ (BLD). It is likely that nitrate supplied to the surface layer from the thermocline would have been immediately removed via efficient nutrient uptake by small-celled phytoplankton [*Chisholm*, 1992]. Data from nutrient uptake experiments conducted on the same research cruise (C. Williams, unpublished data, 2013) indicate that the surface layer community was capable of assimilating up to 0.1 mmol m⁻³ h⁻¹ of nitrate. Assuming an approximate 10 m thick surface layer, this is equivalent to a depth integrated uptake rate of approximately 1 mmol m⁻² h⁻¹, and thus any additional nitrate supplied via turbulent fluxes would not have been captured in our observations. However, it is important to note that the estimates of PP used in our calculations are based on bottle measurements of PP. The phytoplankton community would have been isolated from transient nutrient fluxes, and thus bottle measurements are likely to underestimate the rate of PP at the SCM. Additionally, estimating nitrate concentrations based on density could introduce some uncertainty to our flux calculations, as phytoplankton can assimilate nutrients on relatively short timescales compared to changes in the density-nitrate relationship [e.g., *Lucas et al.*, 2011]. However, the density-nitrate gradient varied by less than 1 mmol m⁻⁴ throughout the VMP time series.

4. Summary

[14] Shelf seas are an important global carbon sink, with primary production in the SCM thought to account for a significant fraction of the carbon fixation occurring there [*Kitidis et al.*, 2012]. In order for carbon fixation to be accurately predicted in shelf seas, biophysical models need to incorporate the effect of wind-driven inertial oscillations, which as we have demonstrated, can potentially supply large, intermittent fluxes of nutrients into the euphotic zone.

Additionally, these large, intermittent mixing events are likely to erode and export carbon from the SCM, removing particulate organic carbon from the euphotic zone and transporting it to the BML. The importance of high temporal resolution sampling of turbulence in order to fully capture and quantify the importance of these short-lived wind-driven mixing events is clear. It is possible that some excess nitrate supplied to the base of the thermocline may reach the nitrate limited surface community, though the evidence suggests that nitrate may be assimilated more rapidly than the traditional sampling resolution for nutrients.

[15] The overall contribution of wind-driven mixing events to annual carbon fixation in the Celtic Sea can be estimated by approximating how often this mixing mechanism might occur through a typical stratified season. Using wind data from 10 successive summers in the Irish Sea, *Sherwin* [1987] estimated that wind-driven inertial oscillations may occur every 2 weeks during the summer period (120 days). This is equivalent to approximately nine wind-driven inertial events occurring every summer, with each event potentially supplying 22 (2 to 81) mmol m⁻² d⁻¹ of nitrate to the SCM. The total supply of nitrate to the SCM during summer via wind-driven inertial oscillations would therefore be 197 (19 to 728) mmol m⁻² y⁻¹, with the potential to support 15 (1.5 to 58) g C m⁻² y⁻¹ of new production annually in the SCM, respectively. Measurements of the depth integrated daily total PP from the Celtic Sea [*Hickman et al.*, 2012] equate to an annual summer total PP estimate of 21 to 46 g C m⁻² y⁻¹. Therefore, we can estimate that between approximately 33% and 71% of the total summer primary production is supported by wind-driven fluxes of nitrate-rich deep water into the base of the thermocline. This finding implies that up to 71% of the summer PP may be unaccounted for in models that do not simulate the mixing associated with inertially generated shear spikes correctly, either due to insufficiently resolved wind forcing or poor parameterization of thermocline mixing.

[16] The findings here have shown that the maintenance of and production in the SCM is likely to be dependent on wind for the nitrate supply which sustains it. The frequency of wind events is determined by the position of the Jet Stream, and as our climate changes, the position of the storm track is expected to be altered [*Hu and Wu*, 2004]. Thus, the frequency and intensity of storms over the Northwest European Shelf Seas may change, impacting on the number and seasonality of the intermittent inertial mixing events. We have demonstrated that wind-driven inertial oscillations are an important mixing mechanism that need to be considered in order to gain accurate global carbon fixation estimates.

[17] **Acknowledgments.** The authors would like to thank the UK Natural Environmental Research Council, the funding from which made this research possible. The comments from two anonymous reviewers and the Editor (P. Stratton) greatly improved the paper, and the authors would like to thank them also.

[18] The Editor thanks Vassilis Kitidis and an anonymous reviewer for their assistance in evaluating this paper.

References

- Borges, A. V., B. Delille, and M. Frankignoulle (2005), Budgeting sinks and sources of CO₂ in the coastal ocean: Diversity of ecosystems counts, *Geophys. Res. Lett.*, 32, L14601, doi:10.1029/2005GL023053.
- Borges, A. V., L.-S. Schiettecatte, G. Abril, B. Delille, and F. Gazeau (2006), Carbon dioxide in European coastal waters, *Estuarine Coastal Shelf Sci.*, 70, 375–387.

- Burchard, H., and T. P. Rippeth (2009), Generation of bulk shear spikes in shallow stratified tidal seas, *J. Phys. Oceanogr.*, *29*, 969–985, doi:10.1175/2008JPO4074.1.
- Chisholm, S. W. (1992), Phytoplankton size, in *Primary Productivity and Biogeochemical Cycles in the Sea*, edited by P. G. Falkowski and A. D. Woodhead, pp. 213–237, Plenum Press, New York.
- Efron, B., and G. Gong (1983), A leisurely look at the bootstrap, the jackknife, and cross-validation, *Am. Stat.*, *37*, 36–48.
- Evans, C. A., J. E. O'Reilly, and J. P. Thomas (1987), A handbook for the measurement of chlorophyll *a* and primary production, in *Biological Investigations of Marine Antarctic Systems and Stocks (BIOMASS Scientific Series)*, vol. 8, edited by S. Z. El-Sayed, 114 pp., Sci. Committee on Antarct. Res. and Sci. Committee on Oceanic Res., Scott Polar Res. Inst., Cambridge, U. K.
- Frankignoulle, M., and A. V. Borges (2001), European continental shelf as a significant sink for atmospheric carbon dioxide, *Global Biogeochem. Cycles*, *15*, doi:10.1029/2000GB001307.
- Hickman, A. E., C. M. Moore, J. Sharples, M. I. Lucas, G. H. Tilstone, V. Krivtsov, and P. Holligan (2012), Primary production and nitrate uptake within the seasonal thermocline of a stratified shelf sea, *Mar. Ecol. Prog. Ser.*, *463*, 39–57.
- Hu, Z. Z., and Z. H. Wu (2004), The intensification and shift of the annual North Atlantic Oscillation in a global warming scenario simulation, *Tellus A*, *56*, 112–124.
- Itsweire, E. C., and K. N. Hellend (1989), Spectra and energy transfer in stably stratified turbulence, *J. Fluid Mech.*, *207*, 419–452.
- Jahnke, R. A. (2010), Global synthesis, in *Carbon and Nutrient Fluxes in Continental Margins: A Global Synthesis*, edited by K. K. Liu et al., pp. 597–615, Springer-Verlag, Berlin, Heidelberg.
- Kitidis, V., et al. (2012), Seasonal dynamics of the carbonate system in the western English Channel, *Cont. Shelf Res.*, *42*, 30–40.
- Knight, P. J., M. J. Howarth, and T. P. Rippeth (2002), Inertial currents in the Northern North Sea, *J. Sea Res.*, *47*(3/4), 199–208.
- Lucas, A. J., P. J. S. Franks, and C. L. Dupont (2011), Horizontal internal-tide fluxes support elevated phytoplankton productivity over the inner continental shelf, *Limnol. Oceanogr. Fluids Environ.*, *1*, 56–74, doi:10.1215/21573698-1258185.
- Lucas, A. J., G. C. Pitcher, T. A. Probyn, and R. M. Kudela (2013), The influence of diurnal winds on phytoplankton dynamics in a coastal upwelling system off southwestern Africa, *Deep Sea Res. II*, in press.
- Pollard, R. T. (1980), Properties of near-surface inertial oscillations, *Am. Meteorol. Soc.*, *10*, 385–398.
- Redfield, A. C. (1958), The biological control of chemical factors in the environment, *Am. Sci.*, *46*, 205–221.
- Rippeth, T. R. (2005), Mixing in seasonally stratified shelf seas: A shifting paradigm, *Philos. Trans. R. Soc.*, *363*, 2837–2854.
- Rippeth, T. R., J. H. Simpson, E. Williams, and M. E. Inall (2003), Measurements of the rates of production and dissipation of turbulent kinetic energy in an energetic tidal flow: Red Wharf Bay revisited, *J. Phys. Oceanogr.*, *33*(9), 1889–1901.
- Rippeth, T. P., M. R. Palmer, J. H. Simpson, N. R. Fisher, and J. Sharples (2005), Thermocline mixing in summer stratified continental shelf sea, *Geophys. Res. Lett.*, *32*, L05602, doi:10.1029/2004GL022104.
- Rippeth, T. P., P. J. Wiles, M. R. Palmer, J. Sharples, and J. Tweddle (2009), The diapycnal nutrient flux and shear-induced diapycnal mixing in the seasonally stratified western Irish Sea, *Cont. Shelf Res.*, *29*, 1580–1587.
- Sharples, J., C. M. Moore, T. R. Rippeth, P. M. Holligan, D. J. Hydes, N. R. Fisher, and J. Simpson (2001), Phytoplankton distribution and survival in the thermocline, *Limnol. Oceanogr.*, *46*, 486–496.
- Sharples, J., et al. (2007), Spring-neap modulation of internal tide mixing and vertical nitrate fluxes at a shelf edge in summer, *Limnol. Oceanogr.*, *52*, 1735–1747, doi:10.4319/lo.2007.52.5.1735.
- Sherwin, T. J. (1987), Inertial oscillations in the Irish Sea, *Cont. Shelf Res.*, *7*, 191–213.
- Thomas, H., Y. Bozec, K. Elkalay, and H. J. W. de Baar (2004), Enhanced open ocean storage of CO₂ from shelf sea pumping, *Science*, *304*, 1005–1008, doi:10.1126/science.1095491.
- Tweddle, J. F., J. Sharples, M. R. Palmer, K. Davidson, and S. McNeil (2013), Enhanced nutrient fluxes at the shelf sea seasonal thermocline caused by stratified flow over a bank, *Prog. Oceanogr.*, in press.
- van Haren, H., L. Maas, J. T. F. Zimmerman, H. Ridderinkhof, and H. Malschaert (1999), Strong inertial currents and marginal internal wave stability in the central North Sea, *Geophys. Res. Lett.*, *26*, 2993–1996.
- Williams, C. A. J., J. Sharples, M. Green, C. Mahaffey, and T. P. Rippeth (2013), The maintenance of the subsurface chlorophyll maximum in the western Irish Sea, *Limnol. Oceanogr. Fluids Environ.*, *3*, 61–73.
- Wollast, R. (1998), Evaluation and comparison of the global carbon cycle in the coastal zone and in the open ocean, in *The Sea*, vol. 10, edited by K. H. Brink and A. R. Robinson, pp. 213–252, John Wiley, New York.